ON THE SYMPLECTIC STRUCTURE OF THE PRIMARY VISUAL CORTEX

ALESSANDRO SARTI, GIOVANNA CITTI, AND JEAN PETITOT

Abstract *We propose to model the functional architecture of the primary visual cortex V1 as a principal fiber bundle where the 2-dimensional retinal plane is the base manifold and the secondary variables of orientation and scale constitute the vertical fibers over each point as a rotation-dilation group. The total space is endowed with a natural symplectic structure neurally implemented by long range horizontal connections. The model shows what could be the deep structure for both boundary and figure completion and for morphological structures such as the medial axis of a shape.*

1. INTRODUCTION

There has been recently new applications of differential geometry to neurophysiology of visual perception. In particular, it has been shown in [40] , [41] and [9] that the functional architecture of the area V1 of the primary visual cortex can be geometrically modeled as a 3-dimensional structure $V = M \times P$, where the 2-dimensional retinal plane M is the base manifold and the secondary variable of orientation constitutes the fiber P over each point.

Even if V1 is concretely a 2-dimensional neural layer, it implements $n > 2$ degrees of freedom and is thus abstractly of dimension $n > 2$. This difference between the physical concrete and the geometrical abstract dimensions correspond to what Hubel called an "engrafting" of variables:

> "What the cortex does is map not just two but many variables on its two-dimensional surface. It does so by selecting as the basic parameters the two variables that specify the visual field coordinates (distance out and up or down from the fovea), and on this map it engrafts other variables, such as orientation and eye preference, by finer subdivisions." (Hubel [23], p. 131)

The total space V of the fiber bundle modeling V1 is endowed with a natural *contact* structure neurally implemented by long range horizontal connections. It is possible to hypothesize that this fundamental contact structure (making V1 an implementation of the space of *1-jets* of curves in M) is at the basis of the *contour integration* process.

Now it is well known that contact structures can be extended to *symplectic* structures by adding a new dimension corresponding to the possibility of changing *scale* at every point of M, that is of treating scale as a gauge.

In [9] the secondary variable of orientation constitutes the vertical fibers over each point as a rotation group. Here we will thus propose to add the scale dimension

A. Sarti and G. Citti: University of Bologna, J. Petitot: EHESS and CREA, Ecole Polytechnique, Paris.

to the model [9] and to model the functional geometry of V1 as a principal fiber bundle G where the 2-dimensional retinal plane M is again the base manifold and the secondary variables of orientation and scale constitute now the fibers over each point as a rotation-dilation group. In terms of Hubel's engrafted variables our model engrafts therefore two variables: orientation and scale. The total space will be endowed with a natural symplectic structure also neurally implemented by long range horizontal connections.

Moreover we will show how this symplectic structure can be naturally deduced from the filtering of the optical signal by the receptive fields of visual neurons and their functional architecture.

Our model naturally integrates several features of the visual cortex observed in experiments of neurophysiology, psychophysics and neuroimaging.

We start from the well known observation that the set of simple cells receptive profiles (RPs) is generated by the action of the affine group of the visual plane on a Gabor mother function.

Each hypercolumn of simple cells RPs, defined at a retinal point (x, y), forms a 2-dimensional subgroup of rotations-dilations. This structure is identically repeated for every point of the retina, and can therefore be considered as a fiber of the 4-dimensional principal bundle.

Then we show that the neural process of *maximal selectivity* due to intracortical short range inhibitory connections internal to hypercolumns selects in each case a section of the fibration. This mechanism will be described as the lifting of boundaries in M to curves in V1 and whole figures in M to surfaces in V1.

From the neurophysiological point of view, there is evidence of connections between simple cells belonging to different hypercolumns. These neural connections are what neurophysiologists call long range horizontal connections. They implement what geometers call a *connection* operating a *parallel transport* between fibers of a bundle.[1] This latter connection (in the geometric sense) can be expressed in terms of a symplectic form on the 4-dimensional principal bundle G, introducing on it what is called a *complex structure*.

It was already shown in [40], [9] that the integral curves of the natural contact structure in the 3-dimensional fiber bundle V is a mathematical representation of the *association field* of Field, Hayes and Hess ([17]). In our model here, the integral curves of the symplectic structure model more finely the connectivity pattern between simple cells in V1, as observed by electrophysiological experiments. In other words, the symplectic structure introduces a system of natural coordinates in the 4-dimensional space $\mathbb{C}^2$ which is implemented by neural connectivity.[2] Notice that many of the anatomical and functional features we will discuss and model are common to most mammals, nevertheless we will refer particularly to features experimentally found in tree shrew.

We also refer to the following results, for a theoretical description of the functional architecture of the striate cortex [6], [7], [48], [49], [2], [3].

In this paper we model the cortex as a cotangent fiber bundle that can be interpreted as a phase space from the physical point of view. This is the natural

---

[1]It must be emphasized that the technical lexicons of neurophysiology and geometry use the same terms "fibers", "connections", etc. in completely different ways. In general the context will eliminate any ambiguity.

[2]$\mathbb{C}^2$ is 2-dimensional over $\mathbb{C}$ but 4-dimensional over $\mathbb{R}$.

space for stochastic dynamical systems. The idealized model we presented can be thought as the deterministic counterpart of these stochastic models.

The paper is organized as follows:

- In section 2 we consider the basic properties of simple cells RPs and outline the group structure underlying the set of cells. We show also how 1-forms can be naturally associated to RPs.
- In section 3 we deepen the group structure and introduce the hypercolumnar structure and the related geometrical concept of a principal fiber bundle.
- In section 4 we prove that maximal selectivity in the hypercolumns explains and justifies the association between RPs and 1-forms.
- In section 5 the "horizontal" connectivity between hypercolumns is considered and the notion of symplectic structure on the fiber bundle is introduced. We define also the associated complex structure.
- In section 6 we present numerical simulations of integral curves of the symplectic structure and compare them with neurophysiological experimental results about long range horizontal connections. We show also that the lifting of images yields Lagrangian manifolds, which explains the well known but enigmatic perceptive relevance of the medial axis of a shape.
- For reader convenience we collected in Appendix A the proof of the main theorem, and in Appendix B the basic definitions of differential geometry instruments used in the paper.

2. The Receptive Profiles of Simple Cells

In this section we define the receptive profiles (RP) of neural cells, make explicit the effects on them of a change of frame in the visual plane and show how to associate to a RP a differential 1-form selecting its preferred orientation.

2.1. **Receptive fields and receptive profiles.** A great variety of cells respond to a stimulus on the retinal plane $M \subset \mathbb{R}^2$. The *receptive field* (RF) of a visual neuron is classically defined as the domain of the retina to which it is connected through the neural connections of the retino-geniculo-cortical pathways (projecting from the retina to the cortex through the lateral geniculate nucleus along the thalamic way) and whose stimulation elicitates a spike response.

In the sequel, we will restrict our models to the RF in this narrow sense. Classically, a RF is decomposed into ON (positive contrast) and OFF (negative contrast) zones according to the type of response to light and dark luminance Dirac stimulations. There exists therefore a *receptive profile* (RP) of the visual neuron, which is simply its impulse response as a filter kernel. It is a function $\Psi(x, y)$ (where x, y are retinal coordinates) $\Psi : M \to \mathbb{R}$ which is defined on the retinal plane M and measures the response (ON / OFF) of the neuron to stimulations at the point (x, y). Sophisticated techniques enable the recording of the level curves of the RPs (see e.g. De Angelis [12]). A light and dark spot or bar is switched on and off at different positions of the RF and the mean response is measured. One uses for instance random sequences of flashes (of 50 ms) distributed over a lattice of 20×20 positions, with $100ms - 1s$ for each response after each flash, and takes the mean value on 10 flashes at each position (white noise analysis). The correlation of the inputs (flashes) with the outputs (spikes) yields the transfert function of the neuron.

It is a classical result of neurophysiology, already strongly emphasized by David Marr [34] in the late 1970s, that the RPs of the retinal ganglion cells are like Laplacians of Gaussians. On the contrary, the simple cells of V1 are strongly oriented, and are often interpreted as Gabor patches (trigonometric functions modulated by a Gaussian).

2.2. **The set of receptive profiles.** The visual plane M will be identified with the plane $\mathbb{R}^2$ endowed with coordinates (x, y) and a fixed frame (∂_x, ∂_y). This is of course a wild idealization and presupposes the choice of an arbitrary global origin $O = (0, 0)$.

When a visual stimulus I of intensity $I(x, y) : M \subset \mathbb{R}^2 \to \mathbb{R}^+$ activates the retinal layer of photoreceptors (identified with the visual field) $M \subset \mathbb{R}^2$, the cells centered at every point (x, y) of M process in parallel the retinal stimulus with their receptive profile $\Psi_{(x,y)}$, which is defined on M.

Each RP acting on a point (x, y) depends upon a preferred direction θ and a scale σ, and it has been observed experimentally that *the set of simple cells RPs is obtained via translations to the point (x, y), rotations of angle θ, and dilations of scale $s = e^\sigma$ from a unique profile, of Gabor type.* This means that there does exist a "mother" profile $\Psi_0(\xi, \eta)$ from which all the observed profiles can be deduced by transformation.

A good formula for Ψ_0 seems to be

$$\Psi_0(\xi, \eta) = e^{-(\xi^2 + \eta^2)} e^{2i\eta}.$$

In figure 1 we represent its even part $e^{-(\xi^2 + \eta^2)} cos(2\eta)$, which will be studied in this paper.

It has to be noted that the receptive profiles $\Psi_{(x,y)}$ are localized in a neighborhood of the point (x, y). Hence, they will be expressed in local coordinates, around the point (x, y), obtained by rotation and dilation of the initial ones. Any vector will then have two representations: coordinates $(\tilde{\xi}, \tilde{\eta})$ in the global frame centered at $(0, 0)$, and (ξ, η) in the local frame centered at (x, y) :

$$(1) \qquad \begin{cases} \xi = e^{-\sigma}\Big((\tilde{\xi} - x) \cos\theta + (\tilde{\eta} - y) \sin\theta \Big) \\[2mm] \eta = e^{-\sigma}\Big(- (\tilde{\xi} - x) \sin\theta + (\tilde{\eta} - y) \cos\theta \Big). \end{cases}$$

Therefore all the observed profiles can be modelled as

$$\Psi_{x,y,\theta,\sigma}(\tilde{\xi}, \tilde{\eta}) = e^{-2\sigma} \Psi_0(\xi, \eta).$$

In this model we consider a uniform distribution of orientations and scales, even if there is a neurophysiological evidence of covariation of scale and orientation [24].

We recall that a change of frames can act on the space M or, by duality, on functions defined on M. Precisely, if A is a transformation of M, it transforms also functions ψ through the formula

$$A\psi(\tilde{\xi}, \tilde{\eta}) = \frac{1}{det(A)} \psi(A^{-1}(\tilde{\xi}, \tilde{\eta})).$$

Accordingly we will denote $A^{-1}_{x,y,\theta,\sigma}$ the transformation defined in (1), and obtain

$$\Psi_{x,y,\theta,\sigma}(\tilde{\xi}, \tilde{\eta}) = (A_{x,y,\theta,\sigma}\Psi_0)(\tilde{\xi}, \tilde{\eta}).$$

The expression of A thus becomes:

$$A_{x,y,\theta,\sigma}(\xi, \eta) = \begin{pmatrix} x \\ y \end{pmatrix} + e^\sigma \begin{pmatrix} \cos(\theta) & -\sin(\theta) \\ \sin(\theta) & \cos(\theta) \end{pmatrix} \begin{pmatrix} \xi \\ \eta \end{pmatrix}.$$

Notice that for simplicity we identify translations in the retinal plane and translations in the cortical layers, neglecting the conformal log-polar retino-cortical mapping. Anyway, the mapping can easily be taken into account by introducing a suitable metric on cortical layers.
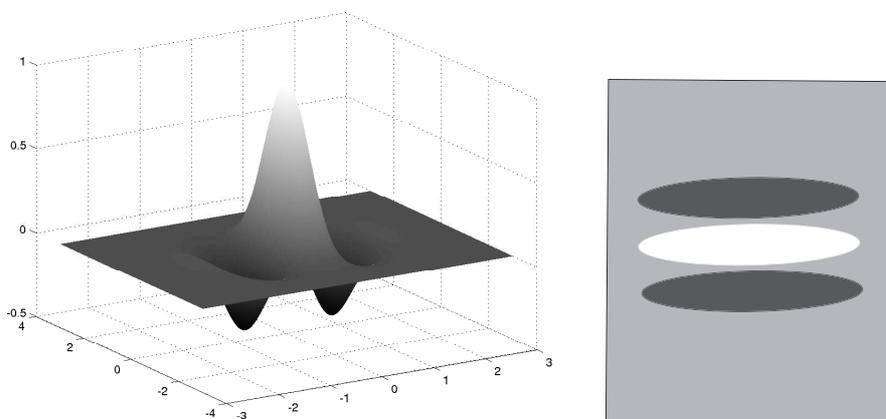
FIGURE 1. A Gabor filter (left) and a schematic representation of its sign (right). Positive sign is in white and negative in black.

2.3. **The output of receptive profiles.** The overall output O of the parallel filtering is given by the integral of the signal $I(x, y)$ times the bank of filters:

$$
\begin{aligned}
O_{(\theta,\sigma)}(x,y) &= \int_M I(\tilde{\xi}, \tilde{\eta}) \Psi_{(x,y,\theta,\sigma)}(\tilde{\xi}, \tilde{\eta}) d\tilde{\xi} d\tilde{\eta} \\
&= \int_M I(\tilde{\xi}, \tilde{\eta}) \Psi_0\Big(A^{-1}_{x,y,\theta,\sigma}(\tilde{\xi}, \tilde{\eta})\Big) \frac{d\tilde{\xi} d\tilde{\eta}}{e^{2\sigma}}
\end{aligned}
$$

(2)

Consequently we can perform a change of variable with respect to the transformation A. We get:

$$O_{(\theta,\sigma)}(x,y) = \int \Psi_0(\xi, \eta) I\big(A_{(x,y,\theta,\sigma)}(\xi, \eta)\big) d\xi d\eta$$

We explicitly note that the linear transformation A acts on the retinal plane M, argument of I. On the contrary the inverse transformation A^{-1} acts on the domain of Ψ_0. This allows us to interpret the domain of Ψ_0 as dual plane, with respect to the retinal plane.

3. FUNCTIONAL GEOMETRY OF HYPERCOLUMNS

3.1. **The hypercolumnar structure.** The hypercolumnar structure organizes the cells of V1 in hypercolumns covering a small chart of the visual field (their receptive field) and corresponding to parameters such as orientation, scale, ocular dominance, direction of movement or color for a fixed retinal position (x, y). The hypercolumnar organization means therefore essentially that to each position (x, y) of the retina M is associated a full exemplar $P_{(x,y)}$ of the space of such "secondary" variables. We restrict here ourselves to orientation θ and scale σ. As we have seen in the introduction, even if the cortical space is a bidimensional layer it "engrafts" secondary variables. Authors in [40] ,[9] proposed a first approximated model with orientation. In [5] the orientation θ is described as a single engrafted secondary variable, in terms of the principal *fiber bundle* of the roto-translation group [3]. Here we will use the same geometrical instruments to propose a new model, which takes into account not only orientation θ but also scale σ, and leads therefore to a 4-dimensional fiber bundle.

3.2. **The fiber $RP_{(x,y)}$ over each retinal point (x, y).** To every fixed point (x, y) of the retinal plane M is associated the complete set of values for orientation θ and scale σ. In other words, for (x, y) fixed, we consider all filters obtained via rotations of an angle θ and dilations of scale e^σ from a fixed one $\Psi_{(x,y,0,0)}$. so that the set of filters over the point (x, y) becomes:

$$
\begin{aligned}
RP_{(x,y)} &= \left\{ \Psi_{(x,y,\theta,\sigma)} : (x,y) \text{ fixed}, (\theta,\sigma) \text{ variable} \right\} \\
&= \left\{ A_{(\theta,\sigma)} \Psi_{(x,y,0,0)} : (\theta,\sigma) \in S^1 \times \mathbb{R} \right\},
\end{aligned}
$$

where we have denoted $A_{(\theta,\sigma)} = A_{(0,0,\theta,\sigma)}$.

3.3. **The group of orientation and scale operating in a hypercolumn.** The set of filters at the point (x, y) is generated as image of

$$
G_2 = \left\{ A_{(\theta,\sigma)} : (\theta,\sigma) \in S^1 \times \mathbb{R} \right\}.
$$

The set G_2 is a trivial commutative group (topologically a cylinder), since, if we apply in sequence two of its elements, we get a new element of it:

$$
A_{(\theta_1,\sigma_1)} A_{(\theta_0,\sigma_0)}(\xi,\eta) = A_{(\theta_0+\theta_1,\sigma_0+\sigma_1)}(\xi,\eta).
$$

Formally, we have a map

$$
\left(A_{(\theta_1,\sigma_1)}, \Psi_{(x,y,\theta,\sigma)} \right) \in G_2 \times RP_{(x,y)} \mapsto \Psi_{(x,y,\theta+\theta_1,\sigma+\sigma_1)} \in RP_{(x,y)}
$$

which formally expresses that the group G_2 acts on the set of all filters RP respecting the fibers $RP_{(x,y)}$. Each filter is obtained from the fixed one via one of these transformations: $RP_{(x,y)}$ is the orbit $G_2 \left(\Psi_{(x,y,0,0)} \right)$.

The change of variable associated to the transformation A acts on the receptive fields $\Psi_{(x,y,\theta,\sigma)}$, as well as on the fixed frame ∂_x, ∂_y, which will be rotated to the vectors

$$
X_1 = e^\sigma \Big(\cos(\theta)\partial_x + \sin(\theta)\partial_y \Big) \quad X_3 = e^\sigma \Big(-\sin(\theta)\partial_x + \cos(\theta)\partial_y \Big).
$$

---

[3]The fiber bundle is a mathematical structure, locally described as a cartesian product $M \times G$, where M models the retinal plane, and G the group of engrafted variables. In the model this expresses the fact that that at every retinal point $(x, y) \in M$ is associated a whole hypercolumn. (We refer to Definition 4 in Appendix B for the precise definition of a fiber bundle).

4. Maximal selectivity and geometrical interpretation of lifting

We come now to one of our central points. Up to now we have described the hypercolumnar structure in terms of differential geometry. Now we introduce the functionality of hypercolumns and particularly the orientation and scale *selectivity*.

In the past years several models have been presented to explain the emergence of orientation and scale selectivity in the primary visual cortex. These models use different combinations of feedforward (thalamic) and feedback (intracortical) signals and consider different involvements of excitatory and inhibitory short range connections (Miller et al. [36], Carandini et al. [8], Bar et al. [1], Shelley et al. [46]). Even if the basic mechanism producing strong orientation selectivity is controversial, nevertheless it is evident that the intracortical circuitry is able to filter out all the spurious directions and to strictly keep the direction of maximum response of the simple cells.

4.1. **The maximization procedure.** Neurophysiologically, orientation and scale selectivity is the action of intracortical short range connections to select the maximum response from the outputs:

$$(3) \qquad O_{(\theta,\sigma)}(x,y) = \int_M I(\tilde{\xi}, \tilde{\eta}) \Psi_{(x,y,\theta,\sigma)}(\tilde{\xi}, \tilde{\eta}) d\tilde{\xi} d\tilde{\eta}, =$$

$$\int_M \Psi_0(\xi_1, \eta_1) I(A_{(x,y,\theta,\sigma)}(\xi_1, \eta_1)) d\xi_1 d\eta_1,$$

where the last integral is obtained with a change of variables.

This maximal selectivity is the simplest mechanism to accomplish the selection from among all different cells responses to effect a lift in the cotangent space. Given an input I, the neural processing associates to each point (x,y) of the retina M a point $(x, y, \bar{\theta}, \bar{\sigma})$ in the cortex, We interpret this mechanism as a lifting into the fiber of the parameter space $\mathbb{R}^2(x,y) \times S^1(\theta) \times \mathbb{R}(\sigma)$ over (x,y). Precisely, the odd part of the filters $\Psi_{(x,y,\theta,\sigma)}$ lifts the boundaries of the image and the even part of the filters lifts the interior of the objects.[4] The odd part has already been studied in [40], [9]. Hence we will focus here on the even part of the filter.

We will denote $(\bar{\theta}, \bar{\sigma})$ the values of the maximal response:

$$O(x, y, \bar{\theta}, \bar{\sigma}) = \max_{(\theta,\sigma)} O(x, y, \theta, \sigma).$$

This maximality condition can be mathematically expressed requiring that the gradient of O with respect to the variables (θ, σ) vanishes at the point $(x, y, \bar{\theta}, \bar{\sigma})$:

$$\nabla^{(\theta,\sigma)} O(x, y, \bar{\theta}, \bar{\sigma}) = 0.$$

We will also require that at the maximum point the Hessian is strictly negatively definite:

$$Hess(O) < 0.$$

For simplicity we will now *reduce to contours*, that is to domains E in M with regular boundaries ∂E, the image I being a cartoon image, formally expressed as a piecewise constant function, which takes only the values 0 or 1. As we will see with the following theorem, a geometrical interpretation of the values of $\bar{\sigma}$ and $\bar{\theta}$ selected

---

[4]Recall that $\Psi_0(\xi, \eta) = e^{-(\xi^2+\eta^2)}e^{2i\eta} = e^{-(\xi^2+\eta^2)}(\cos(2\eta) + i\sin(2\eta))$. The odd part is the sin part and the even part the cos part.

by the maximization procedure just described is that they detect respectively *the distance and the direction of the nearest boundary* (see figure 2).
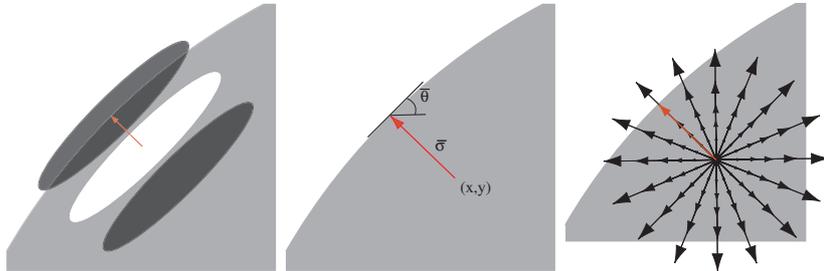
FIGURE 2. The simple cell centered in (x, y) takes the maximal activity $O(x, y, \bar{\theta}, \bar{\sigma}) = \max_{(\theta,\sigma)} O(x, y, \theta, \sigma)$ at a point $\bar{\sigma}$ which is, up to a constant, the logarithm of the distance to the nearest boundary and $\bar{\theta}$ is the direction of this boundary.

Theorem 1. *At first order approximation, for any fixed value of (x, y), the output function $O(x, y, \theta, \sigma)$ reaches a local maximum at the point $\bar{\theta}, \bar{\sigma}$, where $d(\bar{\sigma}) = \frac{1}{\sqrt{2}} e^{\bar{\sigma}}$ denotes the distance of (x, y) from the nearest boundary of the image I, and $\bar{\theta}$ denotes the orientation of this boundary at the point where the distance is achieved.*

The proof is given in the Appendix A.

This theorem ensures that the simple cell selects the couple $(\bar{\theta}, \bar{\sigma})$ in such a way that, X_3 being the vector

$$(4) \qquad\qquad X_3 = e^{\bar{\sigma}} \left(-\sin(\bar{\theta})\partial_x + \cos(\bar{\theta})\partial_y \right),$$

then $(x, y) + \frac{1}{\sqrt{2}} X_3$ belongs to the nearest boundary of I.

4.2. **Simple cells and associated 1-forms.** Let us provide a new interpretation of the action of RPs as filters. A simple cell $\Psi_{\theta,\sigma}(\xi, \eta)$ gives the maximal response for contours with direction θ. We can therefore consider that it *selects* such a direction. But a traditional way to select orientations at points of M is to consider *differential 1-forms* on M. (We refer to Appendix B for the definition of 1- form).

A one form is a linear function, defined on the tangent space, with real values. The form dy, dual of ∂_y, selects the y- component of a tangent vector. Analogously the form obtained by dy, rotating in the inverse direction with respect to A, selects the coefficient of X_3 on $T_{(x,y)}M$, i.e. on the tangent plane of M at the point (x, y):

$$\left(e^{-\sigma}(-\sin(\theta)dx + \cos(\theta)dy) \right)(\xi X_{1|(x,y)} + \eta X_{3|(x,y)}) = \eta.$$

We will therefore associate to any filter $\Psi_{\xi,\eta,\theta,\sigma}$ which is able to select the direction X_3, the 1-form

$$e^{-\sigma}(-\sin(\theta)dx + \cos(\theta)dy)$$

which selects the same direction (see figures 3 and 4).

Due to this correspondance between simple cells and 1-forms selecting their preferential orientation, for every point (x, y) the fiber $RP_{(x,y)}$ of the set of filters
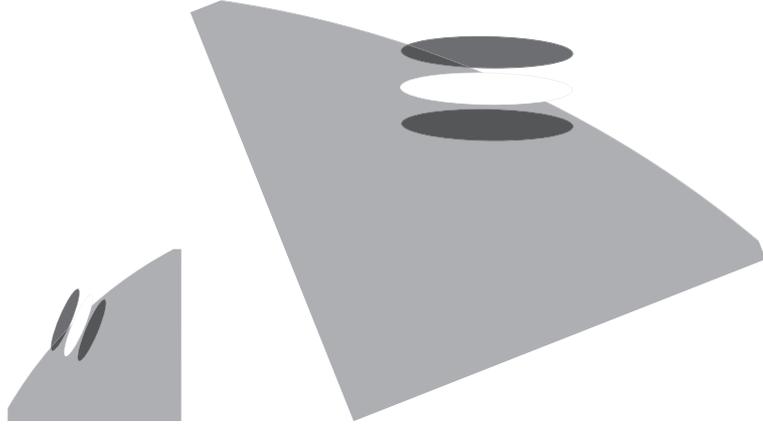
FIGURE 3. The output of a simple cell is equal to the output of the mother filter on an appropriately translated, rotated, and dilated image. This simple cell can therefore be associated with the cotangent vector (the 1-form) deduced from dy by the same transformation.
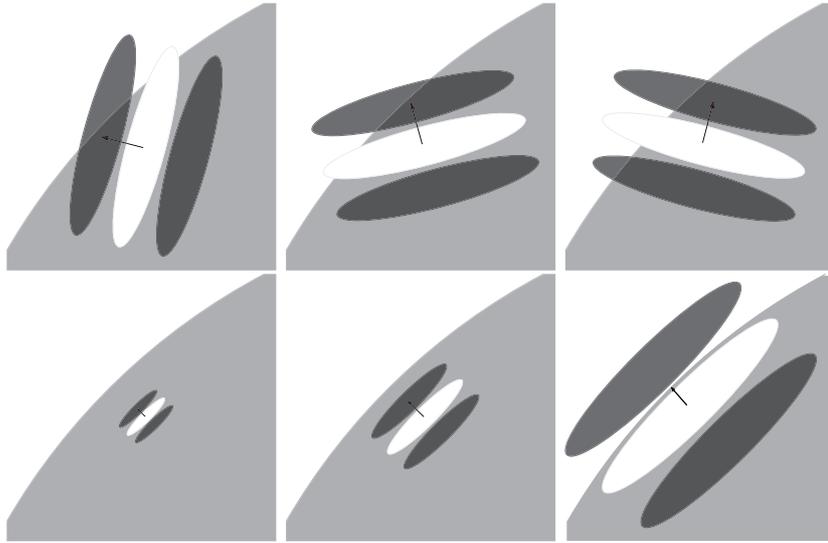
FIGURE 4. Simple cells act on the image as 1-forms (represented in the figure by black arrows), i.e. they select the tangent vector of optimal orientation and scale, where optimality is given by selecting the maximally spiking cell over the fiber.

$\Psi_{(x,y,\theta,\sigma)}$ is made out of elements of the form:

$$(5) \qquad \left\{ \omega_{(\theta,\sigma)} = e^{-\sigma} \left(-\sin(\theta)dx + \cos(\theta)dy \right) : \theta \in [0,\pi], \sigma \in \mathbb{R} \right\}.$$

Using this particular representation, we can say that the coefficients (θ, σ) provide a representation of a co-vector in *log-polar coordinates*, and the elements of this

type completely fill the 2-dimensional cotangent space $T^*_{(x,y)}M$ at (x,y). Hence the fiber over the point (x,y) (the hypercolumn $RP_{(x,y)}$) can be identified with the cotangent space $T^*_{(x,y)}M$ at this point (see figure 5).
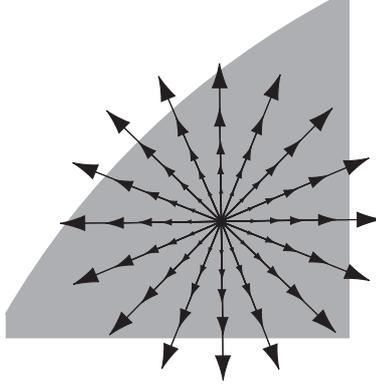
FIGURE 5. A hypercolumn centered in (x,y) acts on the image as a fiber of 1-forms.

4.3. **A field of 1-forms.** We see that the selection of $\bar{\theta}$ and $\bar{\sigma}$ by maximal response of the internal local neural circuitry of the hypercolumn $RP_{(x,y)}$ defines a function

$$\bar{\Sigma}: \quad \begin{array}{ccc} M & \to & RP \\ (x,y) & \mapsto & (x,y,\bar{\theta},\bar{\sigma}) \end{array}$$

Identifying RP with T^*M, $\bar{\Sigma}$ becomes a field of 1-forms (see figure 6). We can interpret this function as the lift the image I in M in the fiber bundle $\pi : RP \to M$.
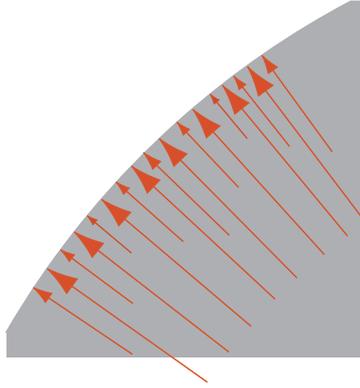
FIGURE 6. The set of maximal responding cells selects a field of 1-forms which lifts the image into V1.

5. Long range neural connections and symplectic structure

In the previous section we have analyzed the selection of an orientation $\bar{\theta}$ and a scale $\bar{\sigma}$ induced in each hypercolumn by its internal circuitry. We will now take into account the relationships between different hypercolumns. We know that these relations are neurophysiologically implemented in long range excitatory intracortical intercolumnar "horizontal" connections. We have seen on the other hand what are the geometrical transformations which relate the fibers $RP_{(x,y)}$ in the fiber bundle RP. [5] In this section we will focus on this double – neurophysiological and geometrical – functional architecture and emphasize the action of the group G of roto-translations and scaling.

5.1. The cotangent bundle associated to the set of receptive fields. We will now make more precise the geometrical structure of the set of all hypercolumns that is implemented in the functional architecture of V1. For every fixed point (x, y), the set $RP_{(x,y)}$ of receptive profiles based at (x, y) has been endowed with a structure of a homogeneous space under the action of a 2-dimensional group G_2.

The set of all hypercolumns is the 4-dimensional fiber bundle

$$RP = \bigcup_{(x,y)} RP_{(x,y)}.$$

If we consider the hypercolumns as the cotangent space at each point (x, y) of M, we associate to the bundle RP the cotangent space T^*M with its system of log-polar coordinates:

$$T^*M = \bigcup_{(x,y)} T^*_{(x,y)}M = \bigcup_{(x,y)} \left\{ (x, y, \theta, \sigma) : e^{-\sigma}(-\sin(\theta)dx + \cos(\theta)dy) \in T^*_{(x,y)}M \right\}.$$

It is clear by definition that any element in the cotangent bundle is a 4-dimensional vector (x, y, θ, σ) where $(x, y) \in M$, while $(\theta, \sigma) \in T^*_{x,y}(M)$ are the coordinates in the cotangent plane at the point (x, y).

The group law G_2 defined on $RP_{(x,y)}$ together with the group law defined on the base space M define a group law on the whole bundle. This group G is

$$G \simeq \left\{ A_{(x,y,\theta,\sigma)} : (x, y, \theta, \sigma) \in \mathbb{R}^2 \times S^1 \times \mathbb{R} \right\}$$

For reader convenience we compute here the group law. Calling

$$r_\theta = \begin{pmatrix} \cos(\theta) & -\sin(\theta) \\ \sin(\theta) & \cos(\theta) \end{pmatrix},$$

and applying in sequence two transformations we get:

$$
\begin{aligned}
A_{(x,y,\theta,\sigma)} A_{(x_1,y_1,\theta_1,\sigma_1)}(\xi, \eta) &= A_{(x,y,\theta,\sigma)}\left(\begin{pmatrix} x_1 \\ y_1 \end{pmatrix} + e^{\sigma_1} r_{\theta_1} \begin{pmatrix} \xi \\ \eta \end{pmatrix} \right) \\
&= \begin{pmatrix} x \\ y \end{pmatrix} + e^\sigma r_\theta \left(\begin{pmatrix} x_1 \\ y_1 \end{pmatrix} + e^{\sigma_1} r_{\theta_1} \begin{pmatrix} \xi \\ \eta \end{pmatrix} \right) \\
&= \begin{pmatrix} x \\ y \end{pmatrix} + e^\sigma r_\theta \begin{pmatrix} x_1 \\ y_1 \end{pmatrix} + e^{\sigma+\sigma_1} r_{\theta+\theta_1} \begin{pmatrix} \xi \\ \eta \end{pmatrix} \\
&= A_{(x_2,y_2,\theta_2,\sigma_2)}(\xi, \eta)
\end{aligned}
$$

---

[5]See Appendix B for the definition of a fiber bundle and a fiber.

with

(6) $\sigma_2 = \sigma + \sigma_1, \quad \theta_2 = \theta + \theta_1, \quad \begin{pmatrix} x_2 \\ y_2 \end{pmatrix} = \begin{pmatrix} x \\ y \end{pmatrix} + e^\sigma r_\theta \begin{pmatrix} x_1 \\ y_1 \end{pmatrix}.$

We emphasize again that the composition is *not* commutative.

5.2. Horizontal long range connections and the tangent space to the cotangent plane.

The "vertical" structure of hypercolumns lifts retinal points to cortical ones but it is largely non sufficient to implement a *global coherence*, for which the visual system must be able to *compare* two retinotopically neighboring fibers $RP_{(x_a,y_a)}$ and $RP_{(x_b,y_b)}$ over two neighboring points a and b of M. This problem has been solved at the empirical level by the discovery of "horizontal" cortico-cortical connections (see e.g. [11]). Horizontal connections are long ranged (up to 6-8 mm) and connect cells of approximately *the same orientation* . In distant hypercolumns this allows curved contents of connection fields that have been modeled quantitatively by Ben Shahar [2]. To detect them (see e.g. Ts'o et al. [50]), one can (i) measure the correlations between cells belonging to different hypercolumns; (ii) compare the preferred orientation of a reference cell with the preferred orientation of other cells; (iii) compute cross-correlograms. One verify that cells with neighboring orientations are strongly correlated while cells with sufficiently different orientations are decorrelated.

The key experimental fact is that, while short range connections inside a hypercolumn are isotropic, long range horizontal connections are on the contrary highly *anisotropic* and restricted to cells sharing essentially the same orientation. These two different types of connections implement two different levels of structure: (i) the short range connections implement the local triviality of the fibration $\pi : RP \to M$, while (ii) the long range connections implement a richer structure.

Long range horizontal cortico-cortical connections insure the large scale coherence of retinotopy. Without them, neighboring hypercolumns would become functionally independent and retinotopy would lose any immanent reality for the system itself. That cortico-cortical connections connect neurons of essentially the same orientation in different hypercolumns means that the system is able to know, for (x', y') different from (x, y), if an orientation θ at (x, y) is approximatively the same as an orientation θ' at (x', y').

The direction of the motion between points in the cotangent bundle T^*M belongs to the tangent space to the cotangent space. Since (x, y, θ, σ) are coordinates for T^*M, then $(\partial_x, \partial_y, \partial_\theta, \partial_\sigma)$ is a tangent frame at the origin. On the other side the group G acts on T^*M, and the differential of the left traslation L_g of G by g (that is the map $h \mapsto gh$ of G onto itself) allows to transport the standard basis of T_0G to a *left invariant* basis at any other point of the space. A direct computation shows that this left invariant basis is precisely:

$$\begin{cases} X_1 = e^\sigma \left(\cos(\theta)\partial_x + \sin(\theta)\partial_y \right) \\ X_2 = \partial_\theta \\ X_3 = e^\sigma \left(-\sin(\theta)\partial_x + \cos(\theta)\partial_y \right) \\ X_4 = \partial_\sigma \end{cases}$$

The fact that the standard basis $(\partial_x, \partial_y, \partial_\theta, \partial_\sigma)$ is *not* left invariant manifests the crucial phenomenon of *non holonomy*.

5.3. **The symplectic structure and the scale as a gauge field.** We will now consider another classical stucture defined on the cotangent bundle T^*M, namely its *symplectic structure*.[6] Indeed for every σ we have selected as fundamental 1-form the 1-form defined in [9] and [41] :

$$\omega = e^{-\sigma}\left(-\sin(\theta)dx + \cos(\theta)dy\right).$$

The subspace $V = \mathbb{R}^2(x,y) \times S^1(\theta) \times \{\sigma\}$, associated to the 1-form for a scale σ, is a *contact structure*. We take then as symplectic form on T^*M the 2-form $d\omega$ obtained by differentiating ω with respect to all its variables. The symplectic 2-form $d\omega$ writes:

$$
\begin{aligned}
d\omega &= \left(e^{-\sigma}\cos(\theta)dx + e^{-\sigma}\sin(\theta)dy\right) \wedge d\theta \\
&\quad \left(-e^{-\sigma}\sin(\theta)dx + e^{-\sigma}\cos(\theta)dy\right) \wedge d\sigma \\
&= \omega_1 \wedge \omega_2 + \omega_3 \wedge \omega_4,
\end{aligned}
$$

where ω_i is the dual form of X_i. This form can be identified with the *left invariant* 2-form deduced by left translations from the standard 2-form on G at 0:

$$dx \wedge d\theta + dy \wedge d\sigma.$$

5.4. **The complex structure.** It is well known that every symplectic structure induces a *complex structure*. Let B be the matrix associated to the symplectic form $d\omega$ defined by $d\omega(X, X') = \langle BX, X'\rangle$ [7] for every pair (X, X') belonging to the tangent plane $T_{(x,y,\theta,\sigma)}G$:

$$
\begin{cases}
X = \xi\partial_x + \eta\partial_y + \vartheta\partial_\theta + \varsigma\partial_\sigma \\
X' = \xi'\partial_x + \eta'\partial_y + \vartheta'\partial_\theta + \varsigma'\partial_\sigma
\end{cases}
$$

We have:

$$
(7) \qquad B = e^{-\sigma}\begin{pmatrix} 0 & 0 & -\cos(\theta) & \sin(\theta) \\ 0 & 0 & -\sin(\theta) & -\cos(\theta) \\ \cos(\theta) & \sin(\theta) & 0 & 0 \\ -\sin(\theta) & \cos(\theta) & 0 & 0 \end{pmatrix}.
$$

By definition of a 2-form we have $d\omega(X, X') = -d\omega(X', X)$, which implies that

$$B^* = -B$$

(where B^* is the transpose of B) since

$$
\begin{aligned}
d\omega(X, X') &= \langle BX, X'\rangle = \langle X, B^*X'\rangle = \langle B^*X', X\rangle \\
&= -d\omega(X', X) = -\langle BX', X\rangle.
\end{aligned}
$$

From this it is clear that $-B^2 = BB^*$ is non negative definite. In our case

$$-B^2 = e^{-2\sigma}I,$$

where I is the identity map. Hence, if we write

$$P = \sqrt{-B^2} = e^{-\sigma}I,$$

and put

$$J = BP^{-1} = e^{\sigma}B,$$

---

[6]See Appendix B for the definition.
[7]$\langle A, B\rangle$ is the scalar product on the tangent planes.

it is clear that $J^2 = -I$, which means that J defines a complex structure. In our case

$$(8) \qquad J = \begin{pmatrix} 0 & 0 & -\cos(\theta) & \sin(\theta) \\ 0 & 0 & -\sin(\theta) & -\cos(\theta) \\ \cos(\theta) & \sin(\theta) & 0 & 0 \\ -\sin(\theta) & \cos(\theta) & 0 & 0 \end{pmatrix}.$$

Through J, all the tangent spaces of $G = \mathbb{R}^2(x, y) \times S^1(\theta) \times \mathbb{R}(\sigma)$ can be identified with $\mathbb{C}^2$.

The complex/symplectic structure naturally associates the vector fields X_1 and $JX_1 = X_2$, and X_3 and $JX_3 = X_4$. The planes $\{X_1, X_2\}$ and $\{X_3, X_4\}$ spanned by X_1, X_2 and X_3, X_4 at a point (x, y, θ, σ) are complex lines in $\big(T_{(x,y,\theta,\sigma)}G, J\big) \simeq \mathbb{C}^2$.

6. Filtering, symplectic geometry and shape analysis

6.1. **Integral curves of special vector fields.** Viewed in V with $\sigma = \sigma_0$, $\{X_1, X_2\}$ is the *contact plane* $C_{(x,y,\theta)}V$. The integral curves of the contact structure C starting at a fixed point $(x_0, y_0, \theta_0, \sigma_0)$ are tangent to the contact plane at every point. They are called *contact curves* and write

$$(9) \qquad \gamma'(t) = X_1(\gamma(t)) + k(t)X_2(\gamma(t)), \quad \gamma(0) = (x_0, y_0, \theta_0, \sigma_0),$$

k being a parameter varying in $\mathbb{R}$. In particular for k constant, the solution is

$$\begin{cases} x & = & \frac{1}{k}\left(\sin(kt + \theta_0) - \sin(\theta_0) + kx_0\right) \\ y & = & \frac{1}{k}\left(-\cos(kt + \theta_0) + \cos(\theta_0) + ky_0\right) \\ \theta & = & kt + \theta_0 \\ \sigma & = & \sigma_0 \end{cases}$$

For $k = 0$ its projection on the (x, y) plane is the x axis and for $k \neq 0$ it is a circle of radius $1/k$ tangent to the x axis (see figure 7 left). The emergence of curvature in this context is strictly related to the curve detection model based on curvature in [38].

If we take into account the scale σ, x and y are scaled by e^σ while θ remains the same. Analogously, we can consider the integral curves of the vector fields $X_3 + kX_4$,

$$(10) \qquad \gamma'(t) = X_3(\gamma(t)) + k(t)X_4(\gamma(t)), \quad \gamma(0) = (x_0, y_0, \theta_0, \sigma_0).$$

The solution is

$$\begin{cases} x & = & -\frac{\sin(\theta_0)}{k}e^{\sigma_0}\left(e^{kt} - 1\right) + x_0 \\ y & = & \frac{\cos(\theta_0)}{k}e^{\sigma_0}\left(e^{kt} - 1\right) + y_0 \\ \theta & = & \theta_0 \\ \sigma & = & kt + \sigma_0 \end{cases}$$

Its projection on the (x, y) plane is *independent* of k and orthogonal to the direction θ_0. For k variable the integral curve is the line of slope k in the fixed "vertical" plane $\{X_3, X_4\}$ (see figure 7 right).

The projection of these two classes of integral curves on the base plane (x, y) is plotted in figure 8. Their pattern is in good agreement with the pattern of long range connections found both in neurophysiological and psychophysical experiments. In fact, excitatory connections are confined to two regions, one flaring out along the axis of orientation of the cell (co-axial, in blu), and another confined to a narrow zone extending orthogonally to the axis of orientation (trans-axial, in red). The

co-axial connections are similar to the "association field" proposed by Field, Hayes, Hess [17] and are represented here as integral curves of the fields X_1, X_2 (see also [9]). The symplectic model adds *a second set of trans-axial excitatory connections* which extends orthogonally from the orientation axis of the cell. There is anatomical evidence consistent with the existence of this orthogonal connections ([18], [31], [35], [43], [44]). The trans-axial connections are represented here as integral curves of the fields X_3, X_4. The reason why co-axial connections spread out in a fan, while trans-axial connections are more spatially focused is that the roto-translation fields X_1, X_2 not only don't commute but their commutator is linearly independent from them:

$$[X_1, X_2] = -X_3,$$

while the vectors X_3, X_4 don't commute but their commutator is linearly dependent upon them:

$$[X_3, X_4] = -X_3.$$

Then integral curves of roto-translation fields are not planar (figure 8, left) while integral curves of X_3, X_4 belong to a plane (figure 8, right) whose projection on the (x, y) plane is just a line (red line in figure 8, right).
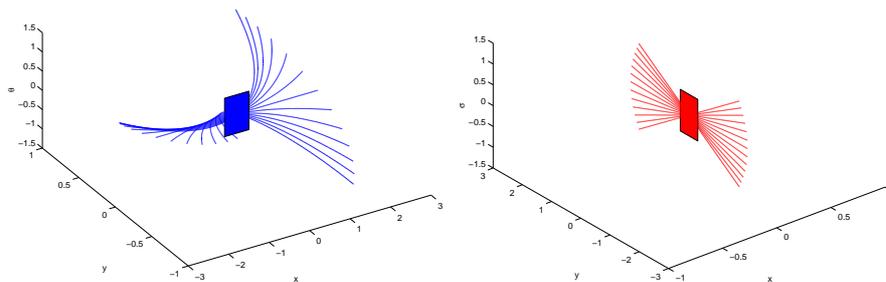
FIGURE 7. Integral curves respectively of the (X_1, X_2) and (X_3, X_4) vector fields.

6.2. **Liftings and Lagrangian manifolds.** Let us now return to the lifted sets described in section 3 and see how we can interpret them relatively to the symplectic structure we have just defined.

We associated to each point (x, y) of the retinal plane, values $\bar{\theta}$ and $\bar{\sigma}$ which we have interpreted as the direction of the nearest boundary and (a function of) the distance from the center of the filter to this boundary. Let us consider the example of figure 9, that of a white ellipse E on a black boundary. The boundary ∂E is lifted as in the contact structure and gives the boundary of the down left ellipse. The gray levels code the values of θ periodically from 0 (black) to π (white). But due to the scale factor σ, we can lift not only the boundary ∂E but *every point* (x, y) of the base. We generate that way a *surface* in G: $\Sigma = \{(x, y, \bar{\theta}, \bar{\sigma})$. As we have shown in section 4, Σ is a part of the extremal surface where the gradient of the output $O(x, y, \bar{\theta}, \bar{\sigma})$ vanishes:

$$\bar{\Sigma} = \left\{(x, y, \bar{\theta}, \bar{\sigma}) : \partial_\theta O(x, y, \bar{\theta}, \bar{\sigma}) = 0, \partial_\sigma O(x, y, \bar{\theta}, \bar{\sigma}) = 0, Hess(O) < 0\right\},$$
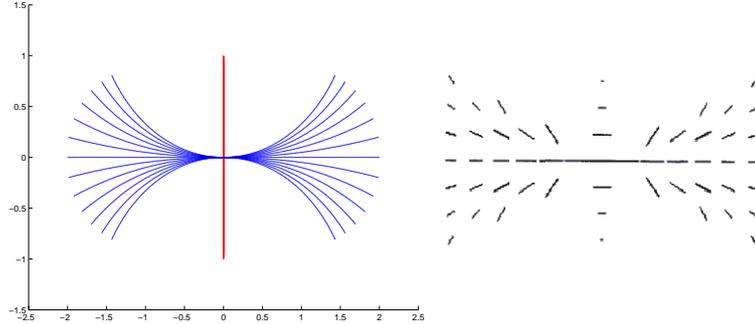
FIGURE 8. The projection of the integral curves of the symplectic structure on the retinal plane (left) reveals the pattern of co-axial and trans-axial connections found by neurophysiological experiments (right, from [47]).

where $Hess$ denote the hessian Matrix of the functin O.

The condition on the Hessian ensures that $\bar{\Sigma}$ is a regular manifold. This locally defines $\bar{\theta}$ and $\bar{\sigma}$ as two functions $\bar{\theta}(x, y)$ and $\bar{\sigma}(x, y)$ on the base plane.
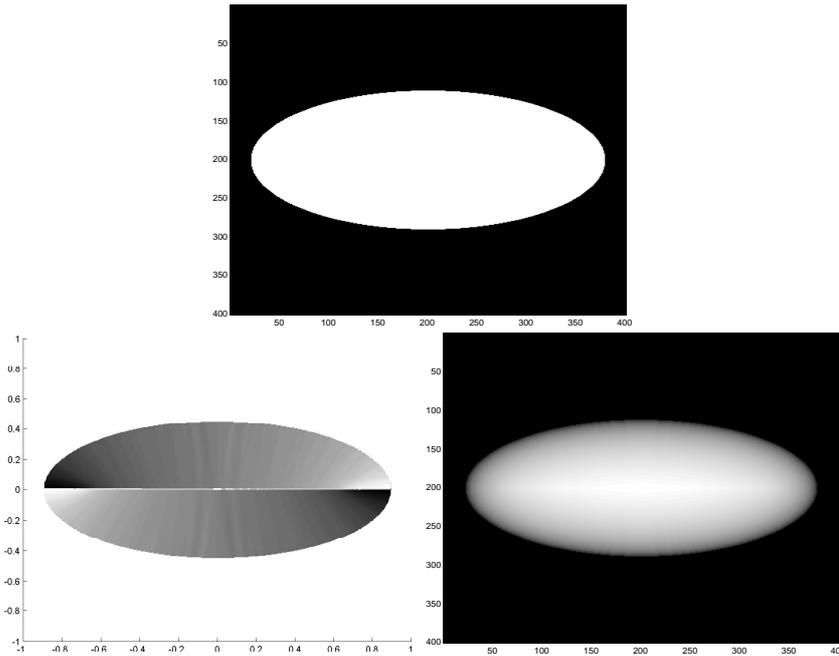
FIGURE 9. Up center: an example of lifting of an ellipse. Down: the corresponding fields of selected orientation $\bar{\theta}$ (left) and scale $\bar{\sigma}$ (right). The exterior structure has been cancelled for graphical reasons.

From the properties of the two functions $\bar{\theta}, \bar{\sigma}$, we can deduce interesting properties of Σ relative to the symplectic structure, at least under the assumptions of

Theorem 1 of section 4. Indeed, according to this theorem $\bar{\theta}(x, y)$ is the direction of the nearest boundary ∂E and $\bar{\sigma}(x, y)$ (up to a factor) the distance of (x, y) to this boundary. This implies that the projections of the level curves of $\bar{\theta}(x, y)$ are orthogonal to the boundary ∂E and dually that the level curves of $\bar{\sigma}(x, y)$ are parallel to ∂E (see figure 10). In other words, *the filtering of the* indicatrix function of the set E *by the family of filters* $\Psi_{(x,y,\theta,\sigma)}$ *realizes the well-known propagation of the boundary by the eikonal equation of geometrical optics*: the boundary propagates as parallel wave fronts and its points generate rays orthogonal to the fronts. We can call it a Huyghens model. The singularities of the propagation generate the so called *"cut locus"* or *symmetry axis* of the shape. The symmetry axis of a shape, which is so fundamental for its morphological analysis, segmentation, and recognition as was shown since Harry Blum's pioneering works (Blum [4]) by René Thom, David Marr, David Mumford, Steve Zucker, James Damon and many others (see Petitot [39] and Kimia [27]), *has therefore a neurophysiological relevance in our model*. It is not surprising since symplectic structures constitute the framework of Hamiltonian mechanics and the Huyghens model (propagation of rays and wave fronts) is universal in Hamiltonian systems. As far as a symplectic structure is neurally implemented in V1 it is natural to observe Hamiltonian structures such as symmetry axes.

Consider now a point (x, y) in the base space M. $\bar{\theta}(x, y)$ and $\bar{\sigma}(x, y)$ are as in figure 10:

$$X_1 = e^{\bar{\sigma}} \left(\cos(\bar{\theta}) \partial_x + \sin(\bar{\theta}) \partial_y \right)$$

is parallel to the orientation of the boundary ∂E at the point of minimal distance $\bar{\sigma}$ and therefore

$$X_1 (\bar{\sigma}) = 0$$

Analogously,

$$X_3 = e^{\bar{\sigma}} \left(-\sin(\bar{\theta}) \partial_x + \cos(\bar{\theta}) \partial_y \right)$$

is orthogonal to the orientation of this nearest boundary and it is constant along this direction $\bar{\theta}$. Therefore:

$$X_3 (\bar{\theta}) = 0$$

From these relations we can deduce that

Theorem 2. *The tangent plane to the surface Σ belongs to the kernel of the symplectic form $d\omega$ at every point $(x, y, \bar{\theta}, \bar{\sigma})$.*

Proof. We compute first the tangent plane to the lifted surface Σ at $(x, y, \bar{\theta}, \bar{\sigma})$. In the basis $\{X_1, \cdots, X_4\}$ it is spanned by the two vectors

$$\begin{cases} X_1 + X_1 \bar{\theta} X_2 + X_1 \bar{\sigma} X_4 \\ X_3 + X_3 \bar{\theta} X_2 + X_3 \bar{\sigma} X_4 \end{cases}$$

On the other side the symplectic 2-form $d\omega$ can be represented as

$$d\omega = \omega_1 \wedge \omega_2 + \omega_3 \wedge \omega_4$$

with $\{\omega_1, \cdots, \omega_4\}$ the dual basis of $\{X_1, \cdots, X_4\}$. Hence, applying the two form to the tangent vectors we get

$$\left(\omega_1 \wedge \omega_2 + \omega_3 \wedge \omega_4 \right) \left(X_1 + X_1 \bar{\theta} X_2 + X_1 \bar{\sigma} X_4, X_3 + X_3 \bar{\theta} X_2 + X_3 \bar{\sigma} X_4 \right) =$$

$$X_3 \bar{\theta} - X_1 \bar{\sigma}.$$
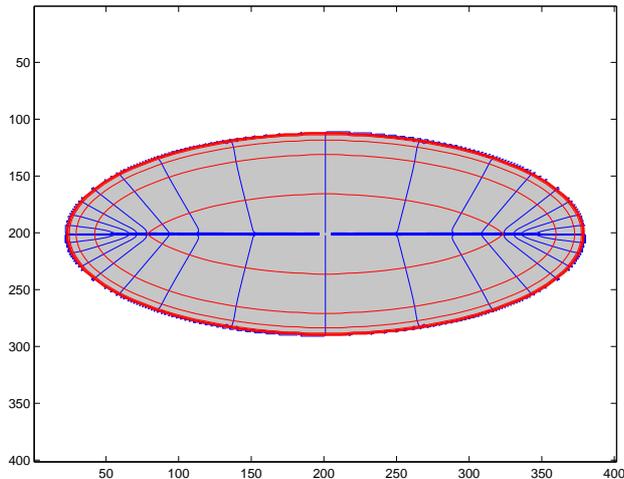
FIGURE 10. Level curves of $\bar{\theta}(x, y)$ (blue) and $\bar{\sigma}(x, y)$ (red).

But as $X_1\bar{\sigma} = X_3\bar{\theta} = 0$, we see that the tangent vector fields annihilate the symplectic form

□

Definition 1. *Let (G, Ω) be a symplectic 4-dimensional manifold. A (smooth) surface Σ of G is called* Lagrangian *if $\Omega \mid_{T\Sigma} \equiv 0$.*

Corollary 1. *The lifted surface Σ is* Lagrangian.

6.3. **Boundaries and objects: 1- and 2-forms.** If we fix the value of the scale σ, we obtain a simplified model, only dependent on orientation, but independent of the scale. The lifted surface simply reduces to a curve Γ lifting the boundary ∂E in the roto-translation group and called the *Legendrian lift* of ∂E and we find again the situation studied in [9]. In this paper it was proved that the tangents to the lifted curve Γ all lie in the so called contact planes which turn out to be the kernels of the 1-form

$$\omega = -\sin(\theta)dx + \cos(\theta)dy.$$

In previous paper [40] , [41] it has been proposed a linearized version of the same form.

The analogous result for surfaces is contained in the previous theorem, since the lifted surface is Lagrangian with respect to the 2-form $d\omega$.

7. CONCLUSION

We have shown how to filter a contour using a family of filters derived from a mother filter whose receptive profile is that of a simple cell of V1. This family is an homogeneous space under the action of the group $G(x, y, \theta, \sigma)$ of translations, rotations, and scaling of the retinal plane M. The horizontal cortico-cortical connections implement the natural $G-$invariant symplectic structure of this space.

We have then shown that the maximal response of the filters to an input contour ∂E computes at every point (x, y) of M the nearest distance $d(\bar{\sigma})$ of (x, y) to ∂E and the orientation $\bar{\theta}$ of ∂E at its nearest point to (x, y). The lifted surface $\Sigma = \{(x, y, \bar{\theta}, \bar{\sigma})\}$ is a Lagrangian surface and realizes the Huyghens model (rays and wave fronts propagation) of the contour ∂E, propagation whose singularities constitute the cut locus (the symmetry axis) of the shape E.

8. Appendix A - Proof of theorem 1

We give a simple sketch of the proof using the fact that I is the indicatrix function of a set E with regular boundary ∂E, i.e. is 1 inside the set E and -1 outside. Hence the gradient ∇I vanishes out of the boundary ∂E.

It is not restrictive to consider a fixed cell $\Psi_{(0,\sigma)}(\xi, \eta)$. As $\Psi_{(0,\sigma)}(\xi, \eta)$ is considered to be defined on the tangent plane $T_O M$, we compute the result up to the first order approximation. Then

$$\Psi_{(0,\sigma)}(\xi, \eta) = \frac{1}{e^{2\sigma}} e^{-(\xi^2+\eta^2)/e^{2\sigma}} \cos(2\eta/e^{\sigma}) \simeq \frac{1}{e^{2\sigma}} e^{-(\xi^2+\eta^2)/e^{2\sigma}} \left(1 - 2\frac{\eta^2}{e^{2\sigma}}\right)$$

But it is trivial to verify that

$$\frac{1}{e^{2\sigma}} e^{-(\xi^2+\eta^2)/e^{2\sigma}} \left(1 - 2\frac{\eta^2}{e^{2\sigma}}\right) = \partial_\eta \left(\frac{1}{e^{2\sigma}} \eta e^{-(\xi^2+\eta^2)/e^{2\sigma}}\right)$$

and therefore, up to first order approximation,

(11) $$\Psi_{(0,\sigma)}(\xi, \eta) \simeq \partial_\eta \left(\frac{\eta}{e^{2\sigma}} e^{-(\xi^2+\eta^2)/e^{2\sigma}}\right)$$

In our case the tangent vector $X_3 = e^{\sigma}\left(-\sin(\theta)\partial_x + \cos(\theta)\partial_y\right)$ reduces to $X_3 = e^{\sigma}\partial_\eta$ at O. Hence, if we denote by $K_{(0,\sigma)}(\xi, \eta)$ the function on $T_O M$

$$K_{(0,\sigma)}(\xi, \eta) = \frac{\eta}{e^{3\sigma}} e^{-(\xi^2+\eta^2)/e^{2\sigma}},$$

we get

$$\Psi_{(0,\sigma)}(\xi, \eta) = e^{\sigma}\partial_\eta \left(\frac{\eta}{e^{3\sigma}} e^{-(\xi^2+\eta^2)/e^{2\sigma}}\right) = X_3\left(K_{(0,\sigma)}(\xi, \eta)\right).$$

Hence the output $O(0, 0, 0, \sigma)$ is given by

$$O(0, 0, 0, \sigma) = \int_M X_3\left(K_{(0,\sigma)}(\xi, \eta)\right) I(\xi, \eta) d\xi d\eta$$

and, integrating by parts, we get

$$O(0, 0, 0, \sigma) = -\int_M K_{(0,\sigma)}(\xi, \eta) X_3\left(I(\xi, \eta)\right) d\xi d\eta$$

since $K_{(0,\sigma)}(\xi, \eta) I(\xi, \eta)$ vanishes at infinity.

Since I is the indicatrix function of E, its gradient ∇I vanishes inside and outside E, and can be represented, as a Dirac mass concentrated on ∂E, with the direction of the outer normal ν of E: $\nabla I = \nu \delta_{|\partial E}$. Then, if $\langle \bullet \mid \bullet \rangle$ is the scalar product, we have $X_3\left(I\right) d\xi d\eta = \langle X_3 \mid \nabla I \rangle = \langle X_3 \mid \nu \rangle \delta_{|\partial E} = $ (since X_3 and ω are dual one of each other) $= \langle \omega, \nu \rangle = \omega(\nu)$. We get finally that

$$O(0, 0, 0, \sigma) = -\int_{\partial E} K_{(0,\sigma)}(\xi, \eta) \omega(\nu) \delta_{|\partial E}.$$

Since ω is the dual form of X_3, ω vanishes for the direction X_1, reaches it maximum $e^{-\sigma}$ for the orthogonal direction X_3 and its minimum $-e^{-\sigma}$ for the opposite direction $-X_3$. The value $\omega(\nu)$ is therefore extremal when the boundary ∂E is of orientation $\theta = 0$.

As for $K_{(0,\sigma)}(\xi, \eta)$ we have

$$K'_{(0,\sigma)}(0, \eta) = \left(-2\eta^2 e^{-2\sigma} + 1\right) e^{-3\sigma - \eta^2/e^{2\sigma}}$$

and $K'_{(0,\sigma)}(0, \eta)$ vanishes for

$$\eta = \frac{1}{\sqrt{2}} e^{\sigma}$$

Up to first order approximation, we can suppose that the regular boundary ∂E is an horizontal line $\eta = cst$. Then

$$
\begin{aligned}
O(0,0,0,\sigma) &= -\int_{\partial E} K_{(0,\sigma)}(\xi,\eta)\omega(\nu)\delta_{|\partial E} \\
&= -\int_{\mathbb{R}} K_{(0,\sigma)}(\xi,\eta)e^{-\sigma}d\xi \\
&= -\sqrt{\pi}\frac{\eta}{e^{3\sigma}}e^{-\eta^2/e^{2\sigma}}.
\end{aligned}
$$

It is proportional to $K_{(0,\sigma)}(0,\eta) = \frac{\eta}{e^{3\sigma}}e^{-\eta^2/e^{2\sigma}}$ and reaches it maximum

$$\sqrt{\pi}\frac{1}{\sqrt{2}}e^{\sigma}\frac{1}{e^{3\sigma}}e^{-\left(\frac{1}{\sqrt{2}}e^{\sigma}\right)^2/e^{2\sigma}} = \sqrt{\frac{\pi}{2}}\frac{1}{e^{(2\sigma + \frac{1}{2})}}$$

when $K_{(0,\sigma)}(0,\eta)$ reaches it minimum.

The integral $O(0,0,0,\sigma)$ will therefore reach its maximum

$$\sqrt{\frac{\pi}{2}}\frac{1}{e^{(2\sigma + \frac{1}{2})}}$$

when $K_{(0,\sigma)}$ attains its maximum on ∂E, and $-X_3$ and ν coincide. The orientation $\theta = 0$ is the orientation of the boundary, while $K_{(0,\sigma)}$ is maximum at the point (ξ, η) which have distance $d(\sigma) = \frac{1}{\sqrt{2}}e^{\sigma}$ to the boundary ∂E. This argument is local, but in order to see that the maximum is reached at the nearest boundary, we fix the direction of Ψ and we vary the scale. Since Ψ has null mean, the integral defining O tends to 0 when the scale tends to 0 and the filter Ψ tends to concentrate on the support of the image I. Hence increasing the value of the scale, the integral increases until the first zero of Ψ cross the boundary of I. At this point the integral start decreasing again. Hence the maximum is reached when θ is the orientation of the nearest boundary. $\square$

9. Appendix B. - Differential geometry instruments

Let us briefly recall the definition of some mathematical concepts used in the paper.

By simplicity we give all definitions in $\mathbb{R}^2$. The definitions in vector spaces of higher dimension is analogous. If the local parametric equation of a curve γ is $(x(t), y(t))$ then its tangent vector at a point $(x(t), y(t))$ will be

$$\vec{X} = (\alpha_1(t), \alpha_2(t)) = (x'(t), y'(t)).$$
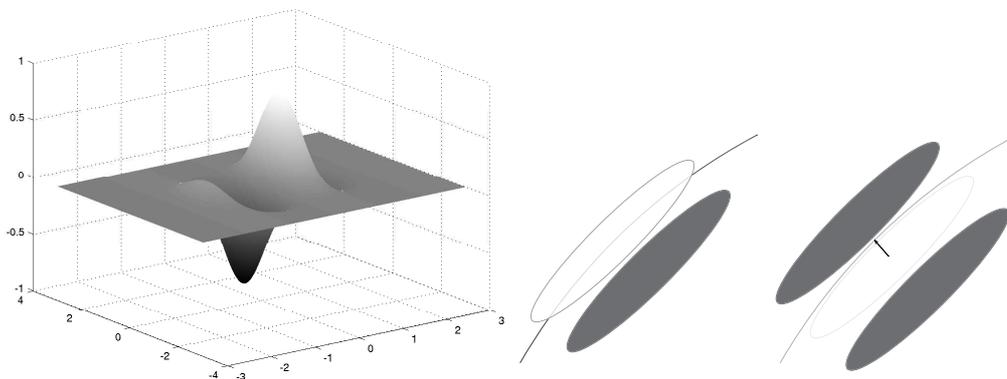
FIGURE 11. The shape of the function $K_{(0,\sigma)}$. Note that, since the derivative of $K_{(x,y,\theta,\sigma)}$ is the even filter $\Psi_{(x,y,\theta,\sigma)}$, then $K_{(x,y,\theta,\sigma)}$ is an odd filter. Left: it reaches its maximum at a distance $d(\sigma) = e^{\sigma}/\sqrt{2}$ from the center. Center: the choice of $K_{(x,y,\theta,\sigma)}$ which maximizes the output O. Recall that the function K has been choosen in such a way that its derivative is the filter $\Psi_{(x,y,\theta,\sigma)}$. Right: the corresponding shape of $\Psi_{(x,y,\theta,\sigma)}$, which vanishes where $K_{(x,y,\theta,\sigma)}$ is maximum.

If we identify the curve γ with the trajectory of a point, the tangent vector $\vec{X}$ describes the direction of the motion at every point.

Definition 2. Tangent space. *The set of tangent vectors is denoted $T_{(x,y)}M$, and it is a plane, called tangent plane at M at the point (x, y).*

At every tangent vector $\vec{X} = (\alpha_1, \alpha_2)$ we can associate the directional derivative along the vector $\vec{X}$, and we denote it with a similar symbol (where ∂_x means $\frac{\partial}{\partial x}$):

$$X = \alpha_1 \partial_x + \alpha_2 \partial_y.$$

With this identification the basis of the tangent space $T_{(x,y)}M$ at (x, y) is (∂_x, ∂_y).

Definition 3. Cotangent space. *Linear functions defined on the tangent space at a point (x, y) are called 1-forms, or cotangent vectors. The set of 1-forms at a point (x, y) is denoted $T^*_{(x,y)}$ and it is a vector space of dimension 2. Its basis is denoted (dx, dy). This means that a general 1-form can be expressed as*

$$\omega = \omega_1 dx + \omega_2 dy.$$

By definition, a form is a function defined on the tangent space, and, being linear the action is formally analogous to a scalar product:

$$\omega(X) = \omega_1 \alpha_1 + \omega_2 \alpha_2.$$

However this operation is called duality, instead of scalar product, since it acts between different spaces: ω_1, ω_2, are coefficients of a 1-form and α_1, α_2 coefficients of a tangent vector.

Example 1. *The simplest example of a 1-form is the differential of a regular function f, which can be represented as*

$$df = \frac{\partial f}{\partial x}dx + \frac{\partial f}{\partial y}dy.$$

Hence it is expressed in terms of the standard basis dx, dy.

Applying the 1-form df to a tangent vector $X = (\alpha_1, \alpha_2)$, we obtain the directional derivative of f, which can be considered the projection of the differential in the direction X.

$$df(X) = \alpha_1 \partial_x f + \alpha_2 \partial_y f.$$

We can as well give a notion which generalize the idea of orthogonal and parallel vectors, using the duality in place of the scalar product. Given a form $\omega = \omega_1 dx + \omega_2 dy$, its dual vector field is the vector field which has the same components: $X = \omega_1 \partial_x + \omega_2 \partial_y$, formally being parallel to ω. The kernel of the 1-form ω is the set of vector X such that

$$\omega(X) = 0.$$

In the model of odd cells we considered the 1- form

$$-\sin(\theta)dx + \cos(\theta)dy.$$

It is easy to see that the vector fields

$$X_1 = \cos(\theta)\partial_x + \sin(\theta)\partial_y, \quad X_2 = \partial_\theta$$

are orthogonal to ω, so that they belong to the kernel of ω.

The kernel of a 1-form is a subset of the tangent plane. For this reason the action of simple cells receptive profiles on the image can be modeled as the selection of tangent vector (to the level lines) by a 1-form. In particular, the vector X_1 which describes the direction of the level lines of the image belongs to the kernel of the form ω.

Up to now we have fixed the point (x, y) and considered the tangent space $T_{(x,y)}$ to M at the point (x, y). We can now vary the point (x, y). The union of all tangent spaces is called the tangent bundle of M:

$$TM = \bigcup_{(x,y) \in M} T_{(x,y)}.$$

A point of the tangent bundle is denoted

$$(x, y, \alpha_1, \alpha_2),$$

where $(x, y) \in M$ and (α_1, α_2) belongs to the tangent space at the point (x, y). Then we have a natural projection

$$\pi : TM \to M \quad \pi(x, y, \alpha_1, \alpha_2) = (x, y).$$

More generally let us now define a fiber bundle, which is the mathematical structure proposed to describe the hypercolumnar structure.

Definition 4. Fiber bundle. *A fiber bundle is defined by two differentiable manifolds M and C, a group G, and a projection π. C and M are called respectively base space and total space.*

The total space is locally described as a cartesian product

$$C = M \times G,$$

meaning that at every point $(x, y) \in M$ is associated a whole copy of the group G, called the fiber. The function π is a surjective differential map, which locally acts as follows

$$\pi : M \times G \to M \quad \pi(x, y, g) = (x, y),$$

where g is an element of G. In the paper the base space is implemented in the retinal space and the total space in the cortical space. Particularly the group G of rotations and scales to the point (x, y) is implement in an hypercolumn over the same point.

Definition 5. Section of a fiber bundle. *A function*

$$\Sigma : (x, y) \to (x, y, \bar{g})$$

defined on the base space M with values in the fiber bundle is called a section of the fiber bundle. In other words a section is the selection of a point on a fiber.

In the model introduced here we associate to each point (x, y) of the retinal plane an orientation and scale value, i.e. a point $(\bar{\theta}, \bar{\sigma})$ in the feature space, defining a section of the cortical bundle

$$\Sigma : (x, y) \to (x, y, \bar{\theta}, \bar{\sigma})$$

The geometrical tools and bundles described up to now can be used to define complex geometrical structures.

Contact geometry is the study of a geometric structure on smooth manifolds given by a hyperplane distribution in the tangent bundle. This hyperplane can be specified by an orthogonal vector, or, more precisely by an orthogonal 1-form:

Definition 6. Contact structure. *A contact structure is an odd dimensional differentiable structure with a 1 form ω, which satisfies a 'maximum non-degeneracy' condition*

$$\omega \wedge (d\omega)^n \neq 0$$

Starting with a contact structure ω a classical way to define a symplectic structure is to multiply ω by a real variable $\omega_1 = \alpha\omega$ and differentiatng ω_1. Note that $\Omega = d\omega_1$ is a 2-form such that $d\Omega = 0$. It can be expressed in terms of the standard basis

$$\Omega = \Omega_{ij} dx_i \wedge dx_j$$

The space is now even-dimensional, since we add the extra variable α. Hence the formal definition of a symplectic structure is the following:

Definition 7. Symplectic structure. *A symplectic form Ω on an even manifold M is a nondegenerate, closed two-form*

$$\Omega = \Omega_{ij} dx_i \wedge dx_j.$$

Explicitly, nondegeneracy of the form means that the matrix Ω_{ij} is a skew-symmetric and non-singular matrix, i.e., with non vanishing determinant. The requirement that Ω is closed, means that

$$d\Omega = 0$$

where d is the exterior derivative.

The simplest example of a symplectic form is

$$\sum_i dx_i \wedge dy_i,$$

in a complex space $\{(x_1 + iy_1 \cdots x_n + iy_n)\}$. In this case the 2-form expresses the coupling of the variables x_i with the correspondent variables y_i in the complex structure.

References

[1] Bar O, H.Sompolinsky, R. Ben-Yishai (1995) Theory of orientation tuning in visual cortex, PNAS 92: 3844-3848.

[2] Ben S (2003) Geometrical computations explain projection patterns of long-range horizontal connections in visual cortex, Neural Comp, 16 (3): 445-476.

[3] Ben S, Zucker S (2004) Geometrical Computations Explain Projection Patterns of Long-RangeHorizontal Connections in Visual Cortex, Neural Comput, 16: 445-476.

[4] Blum H (1973) Biological Shape and Visual Science, Journal of Theoretical Biology, 38: 205-287.

[5] Bosking W, Zhang Y, Schoenfield B, Fitzpatrick D (1997) Orientation selectivity and the arrangement of horizontal connections in tree shrew striate cortex, J. Neurosci, 17 (6): 2112-2127.

[6] Bressloff P C, Cowan J D, Golubitsky M, Thomas P J, Wiener M, (2001) Geometric visual hallucinations, Euclidean symmetry and the functional architecture of striate cortex, Phil. Trans. Roy. Soc., B 40: 299-330.

[7] Bressloff P C, Cowan J D (2003) Functional geometry of local and horizontal connections in a model of V1. J. Physiol. (Paris) 97: 221-236.

[8] Carandini M, Ringach D L (1997) Predictions of a recurrent model of orientation selectivity, Vision Res., 37: 3061-3071.

[9] Citti G, Sarti A (2006) A cortical based model of perceptual completion in the Roto-Translation space, Journal of Mathematical Imaging and Vision, 24 (3): 307-326.

[10] Citti G, Manfredini M, Sarti A (2004) Neuronal Oscillations in the Visual Cortex: $\Gamma-$convergence to the Riemannian Mumford-Shah Functional, SIAM Jornal of Mathematical Analysis, 35 (6): 1394-1419.

[11] Das A, Gilbert C D (1995) Long range horizontal connections and their role in cortical reorganization revealed by optical recording of cat primary visual cortex, Nature, 375: 780-784.

[12] Daugman J G (1985) Uncertainty - relation for resolution in space, spatial frequency and orientation optimized by two dimensional visual cortical filters, J. Opt. Soc. Amer., 2(7): 1160-1169.

[13] De Angelis G C, Ozhawa I, Freeman R D (1995) Receptive-field dynamics in the central visual pathways, Trends Neurosci., 18 (10): 451-458.

[14] Engel A K, Konig P, Gray C M, Singer W (1990) Stimulus dependent neuronal oscillations in cat visual cortex: intercolumnar interaction as determined by cross-correlation analysis, European Journal of Neuroscience, 2: 558-606.

[15] Engel A K, Kreiter A K, Konig P, Singer W (1991) Synchronization of oscillatory neuronal responses between striate and extrastriate visual cortical areas of the cat, PNAS, 88: 6048-6052.

[16] Gilbert C D, Das A, Ito M, Kapadia M, Westheimer G (1996) Spatial integration and cortical dynamics, PNAS, 93 (2): 615-622.

[17] Field D J, Hayes A, Hess RF (1993) Contour integration by the human visual system: evidence for a local Association Field, Vision Research, 33: 173-193.

[18] Fitzpatrick D (1996) The functional organization of local circuits in visual cortex: insights from the study of tree shrew striate cortex, Cerebral Cortex, 6: 329-341.

[19] Gray C M, Konig P, Engel A K, Singer W (1989) Oscillatory responses in cat visual cortex exhibit inter-columnar syncronization which reflects global stimulus properties, Nature, 338: 334-337.

[20] Grossberg S, Mingolla E (1985) Neural dynamics of perceptual grouping: textures, boundaries and emergent segmentations, Perception and Psychophysics, 38 (2): 141-171.

[21] Frégnac Y, Shulz D (1999) Activity-dependent regulation of receptive field properties of cat area 17 by supervised Hebbian learning, J. Neurobiol., 41 (1): 69-82.
[22] Hoffman W C (1989) The visual cortex is a contact bundle, Applied Mathematics and Computation, 32: 137-167.
[23] Hubel D H (1988) Eye, Brain and Vision, Scientific American Library.
[24] Issa N P, Trepel C, Stryker M P (2000) Spatial frequency maps in cat visual cortex. J Neurosci. 22 (22): 8504-8514.
[25] Jones J P, Palmer L A (1987) An evaluation of the two-dimensional Gabor filter model of simple receptive fields in cat striate cortex, J. Neurophysiology, 58: 1233-1258.
[26] Kapadia M K, Ito M, Gilbert C D, Westheimer G (1995) Improvement in visual sensitivity by changes in local context: parallel studies in human observers and in V1 of alert monkeys, Neuron 15: 843-856.
[27] Kimia B B (2003) On the role of medial geometry in human vision, Neurogeometry and Visual Perception (J. Petitot and J. Lorenceau eds), Journal of Physiology-Paris, 97, (2-3): 155-190.
[28] Kovacs I, Julesz B (1993) A closed curve is much more than an incomplete one: effect of closure in figure-ground segmentation, PNAS, 90: 7495-7497.
[29] Kovacs I, Julesz B (1994) Perceptual sensitivity maps within globally defined visual shapes, Nature, 370: 644-646.
[30] Lamme V A F, Super H, Speckreijse H (1998) Feedforward, horizontal and feedback processing in the visual cortex, Curr. Opin. Neurobiol, 8: 529-535.
[31] Lund J, Fitzpatrick D, Humphrey A L (1985) The striate visual cortex of the tree shrew, Cerebral Cortex (Jones E G. Peters A eds), 157-205, New York: Plenum.
[32] Maffei M, Fiorentini A (1976) The unresponsive regions of visual cortical receptive fields, Vision Res., 16: 1131-1139.
[33] Marcelja S (1980) Mathematical description of the response of simple cortical cells, J. Opt. Soc. Amer., 70: 1297-1300.
[34] D. Marr (1982) Vision, Freeman.
[35] Mitchinson G, Crick F (1982) Long axons within the striate cortex : their distribution, orientation, and patterns of connections, PNAS, 79: 3661-3665.
[36] Miller K D, Kayser A, Priebe N J (2001) Contrast-dependent nonlinearities arise locally in a model of contrast-invariant orientation tuning, J. Neurophysiol., 85: 2130-2149.
[37] Nelson S B, Sur M, Somers D C (1995) An emergent model of orientation selectivity in cat visual cortical simples cells, J. Neurosci., 15: 5448-5465.
[38] Parent P, Zucker S W (1989) Trace interference, curvature consistency and curve detection, *IEEE Trans Pattern Analysis and Machine Intelligence*, 11: 823-839.
[39] Petitot J (1989) Modèles morphodynamiques pour la grammaire cognitive et la sémiotique modale, RSSI Canadian Semiotic Association, 9 (1-2-3): 17-51.
[40] Petitot J, Tondut Y (1999) Vers une Neurogeometrie. Fibrations corticales, structures de contact et contours subjectifs modaux, Mathematiques, Informatique et Sciences Humaines, 145, EHESS, CAMS, Paris, 5-101.
[41] Petitot J (2003) The neurogeometry of pinwheels as a sub-Riemannian contact structure, Neurogeometry and Visual Perception (Petitot J, Lorenceau J eds), Journal of Physiology-Paris, 97, (2-3): 265-309.
[42] Priebe N J, Miller K D, Troyer T W, Krukowsky A E (1998) Contrast-invariant orientation tuning in cat visual cortex: thalamocortical input tuning and correlation-based intracortical connectivity, J. Neurosci, 18: 5908-5927.
[43] Rockland K S, Lund J S (1982) Widespread periodic intrinsic connections in the tree shrew visual cortex, Science, 215: 532-534.
[44] Rockland K S, Lund J S (1993) Intrinsic laminar lattice connections in the primate visual cortex, Journal Comp. Neurol, 216 (3): 303-318.
[45] Sarti A, Citti G, Manfredini M (2003) From neural oscillations to variational problems in the visual cortex, Journal of Physiology, 97, (2-3): 87-385.
[46] Shelley M, Wielaard D J, McLaughlin D, Shapley R (2000) A neuronal network model of macaque primary visual cortex (V1): orientation selectivity and dynamics in the input layer $4C_\alpha$, PNAS, 97: 8087-8092.
[47] Yen S C, Finkel L H (1998) Extraction of perceptually salient contours by striate cortical networks, Vision Res., 38, (5): 719-741.

[48] Swindale N V (2004) How different feature spaces may be represented in cortical maps. Network 15: 217-42.

[49] Swindale N V (2000) How many maps are there in visual cortex? Cerebral Cortex 7: 633-43.

[50] Ts'o D, Gilbert C D, Wiesel T N (1986) Relationships between horizontal interactions and functional architecture in cat striate cortex as revealed by cross-correlation analysis, J. Neurosc., 6 (4): 1160-1170.

[51] Worgotter F, Koch C, (1991) A detailed model of the primary visual pathway in the cat: comparison of afferent excitatory and intracortical inhibitory connection schemes for orientation selectivity, J. Neurosci., 11: 1959-1979.